Approximate Solution of Imbibition in Homogeneous Porous Media: A One-Dimensional Analysis

Anuj P. Raval[1],
Research Scholar,
Gujarat Technological University, Ahmedabad-382424, India.
E-Mail: anujravalstar@gmail.com
Dr. Mitesh S. Joshi[2],
Department of Mathematics,
C K Pithawala College of Engineering and Technology,Surat 395007, India.
E-Mail: mitesh.joshi@ckpcet.ac.in

Abstract

This paper is concerned with solving the problem of one-dimensional counter-current imbibition in a homogeneous porous medium. In this research, water and oil are treated as two distinct liquid phases, in which the water is the wetting phase while the oil is the non-wetting phase. This is the common scenario during secondary recovery of oil. During this phase, the fluid behavior is characterized by a nonlinear partial differential equation. To find the solution of this equation, we utilize the Homotopy Analysis Method (HAM), which is a powerful analytical method. Proper boundary conditions are chosen according to the physical phenomenon of the problem. The results are visualized and interpreted with the help of Mathematica 12.0 using graphical plots.

Keywords: Counter Current, Homogeneous Porous Media, Imbibition Phenomena, Homotopy Analysis Method (HAM).

INTRODUCTION

The counter-current imbibition mechanism by which a wetting fluid like water displaces a non-wetting fluid like oil in the opposite direction within porous media is pivotal to oil recovery, especially in fractured reservoirs. Advanced simulation techniques have been used in recent studies to investigate the pore-scale phenomena of this process. For example, Yang et al. [1] have a study utilized phase-field simulations to unveil the sequence of oil-water interaction during counter-current imbibition, presenting the influence of fracture aperture, capillary number, and viscosity ratio on efficiency of recovery. Likewise, work by Zhou et al. [2] utilized pore-scale modeling to appreciate the impact hydraulic fracture propagation has on spontaneous imbibition behavior, offering insight into optimizing fracture networks for better oil recovery.

Homogeneous porous media, with their uniform pore structures, provide consistent fluid flow patterns, and hence they are suitable for the investigation of imbibition processes. A experimental study explored the imbibition behavior in heterogeneous porous media, focusing on the influence of pore structure distribution and boundary conditions on fluid displacement is done by Shuai et al. [3] . Furthermore, studies by Xu et al. [4] used Nuclear Magnetic Resonance (NMR) to investigate fluid occurrence spaces and imbibition oil recovery in the Gulong shale, yielding significant data on fluid distribution in homogeneous porous structures. Parikh et al. [5] established a mathematical model of counter-current imbibition in vertical downward homogeneous porous media and presented solutions to nonlinear partial differential equations that rule the process. Gohil and Meher [6] conducted a study to examine the impact of viscous fluids on counter-current imbibition in heterogeneous porous media using two-phase fluid flow with inclusion of magnetic fields. Suo et al. [7] introduced a numerical approach in modeling imbibition processes involving heterogeneous porous media, stressing consideration of material heterogeneity during simulation.

Imbibition phenomenon is dominated to a large degree by fluid viscosity, interfacial tension, and wettability. Zotelle et al. [8], have study analyzed the effect of viscosity ratios on fluid displacement pattern and recovery efficiency in porous media and demonstrated how optimal viscosity ratios can achieve maximum oil recovery. In addition, Liu et al. [9] conducted research on the surfactant fracturing fluids' imbibition effects in offshore reservoirs and described how surfactants can change rock wettability and decrease interfacial tension to better displace oil .

Nanotechnology has become a potentially useful area for increasing oil recovery by enhancing imbibition. Zhang et al. [10] conducted experimental experiments on spontaneous imbibition-enhanced oil recovery by nanofluids, and they found that silica nanofluids can significantly reduce oil-water interfacial tension and alter rock wettability, thus enhancing oil production. Similarly, studies have also proven that various nanoparticles, including zirconium dioxide and calcium carbonate, possess active roles in oil recovery improvement by altering the wettability of carbonate rocks.

Sophisticated analytical methods have played a crucial role in elucidating the imbibition and oil recovery mechanisms. Meng et al. [11] work on NMR-based measurements were used to track improved oil recovery by imbibition in nonconventional reservoirs, including detailed descriptions of water and oil distributions during the recovery process. Moreover, Wang et al. [12] have studies on the experimental mechanisms for the improvement of oil recovery by spontaneous imbibition with surfactants in tight sandstone reservoirs have indicated the significance of interfacial tension, rock wettability, and core permeability as factors that influence recovery results.

Li [13] gave analytical solutions for the linear counter-current spontaneous imbibition, stressing the need to develop an understanding of fluid dynamics in porous media. In like manner, Tavassoli et al. [14] modeled the oil recovery under counter-current imbibition in water-wet systems, identifying the effect of capillary forces on fluid displacement. Mason et al. [15] carried out experiments on spontaneous counter-current imbibition in core samples, illustrating the effect of core geometry on imbibition efficiency.

Briefly, the synergy of experimental studies, advanced simulation techniques, and nanotechnology has significantly improved our understanding of counter-current imbibition in homogeneous porous media. These results are significant for the development of effective strategies to enhance oil recovery, particularly in complex reservoir conditions.

Supported by this, the present study further investigates the mechanisms of counter-current imbibition using the Homotopy Analysis Method (HAM). HAM is a powerful analytical tool that particularly excels in the solution of nonlinear partial differential equations, which frequently arise in the modeling of two-phase fluid flow in porous media.

As opposed to traditional numerical techniques, HAM provides an adjustable convergence-control parameter, making the solution more accurate and versatile. Utilizing HAM and suitable boundary conditions, this paper suggests finding an accurate and smooth analytical solution of fluid saturation profiles with the ultimate support of effective design and optimization of enhanced oil recovery techniques.

The rest of the paper is organized as follows: Section 2 gives a mathematical formulation of counter-current imbibition process within a homogeneous porous medium. Section 3 presents the Homotopy Analysis Method and its application to solve the problem. Section 4 gives graphical results of concentration profiles using Mathematica (12.0). Finally, Section 5 gives the main conclusions of the manuscript.

Mathematical Formulation

The Fig.1 [5] schematic describes the one-dimensional counter-current imbibition process within a homogeneous porous medium. The region is separated into two different regions: Injected liquid (water) is depicted on the left-hand side, colored light blue. This liquid is the wetting phase and is injected into the porous medium from the left boundary. Original liquid (oil), shown in dark grey on the right-hand side, is the non-wetting phase that originally fills the porous structure.

There is a displacement process at the vertical center boundary, referred to as "imbibition surface ($x = 0$)". Water flows into the porous material and starts replacing the oil by flowing through the porous structure due to capillary action. Pores are described with irregular or branching structures in order to demonstrate the network seen in porous material. The direction of flow is

from left to right, and due to capillary pressure and saturation gradients, oil is driven in the opposite direction, which characterizes the counter-current nature of the flow.

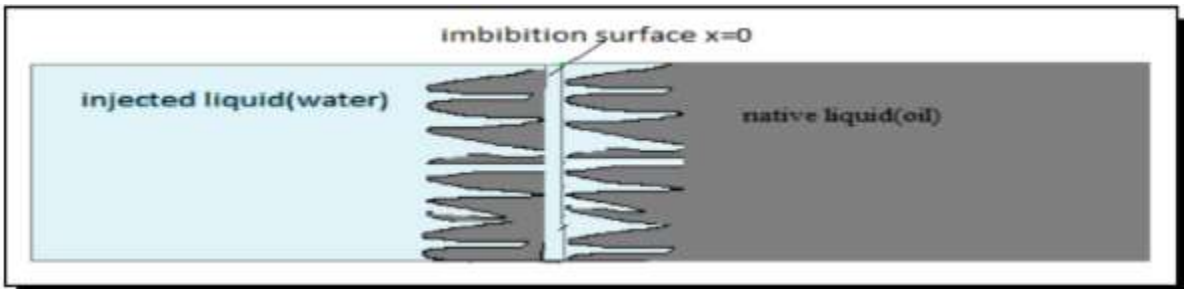

Figure 1. A graphical representation of the process of counter-current imbibition in homogeneous porous media.

Scheidegger [16] highlights that "oil" can serve as a reference for characterizing the seepage velocities of the wetting phase and the non-wetting phase water.

$$\mathcal{V}_w = -\frac{\hbar_w}{\varepsilon_w}\,\mathcal{K}\frac{\partial \mathcal{P}_w}{\partial x} \tag{1}$$

$$\mathcal{V}_o = -\frac{\hbar_o}{\varepsilon_o}\,\mathcal{K}\frac{\partial \mathcal{P}_o}{\partial x} \tag{2}$$

The continuity equations for both the wetting and non-wetting phases are presented by

$$\varphi\frac{\partial S_w}{\partial t} + \frac{\partial \mathcal{V}_w}{\partial x} = 0\,, \varphi\frac{\partial S_o}{\partial t} + \frac{\partial \mathcal{V}_o}{\partial x} = 0 \tag{3}$$

From equation (1),

$$\varphi\frac{\partial S_w}{\partial t} + \frac{\partial}{\partial x}\left(-\frac{\hbar_w}{\varepsilon_w}\,\mathcal{K}\frac{\partial \mathcal{P}_w}{\partial x}\right) \tag{4}$$

$$\varphi\frac{\partial S_o}{\partial t} + \frac{\partial \mathcal{V}_o}{\partial x} = 0 \tag{5}$$

The coordinate x is measured along the axis of the cylindrical medium, with the origin positioned at the imbibition face ,$x = 0$.

The definition of capillary pressure$\mathcal{P}_c$ can be written as Mehta [17]

$$\mathcal{P}_c = \mathcal{P}_o - \mathcal{P}_w \tag{6}$$

The countercurrent interaction between the two phases generates a spontaneous flow that results in the sum of the velocities of water and oil being zero (Scheidegger and Johnson [18]).

Therefore,

$$\mathcal{V}_w + \mathcal{V}_o = 0 \tag{7}$$

$$\mathcal{V}_w = -\mathcal{V}_o \tag{8}$$

From (1) and (2), we get

$$\frac{\hbar_w}{\varepsilon_w}\,\mathcal{K}\frac{\partial \mathcal{P}_w}{\partial x} + \frac{\hbar_o}{\varepsilon_o}\,\mathcal{K}\frac{\partial \mathcal{P}_o}{\partial x} = 0 \tag{9}$$

Substituting for $\mathcal{P}_o$ from equation (6),

$$\frac{\hbar_w}{\varepsilon_w}\,\mathcal{K}\frac{\partial \mathcal{P}_w}{\partial x} + \frac{\hbar_o}{\varepsilon_o}\,\mathcal{K}\frac{\partial}{\partial x}(\mathcal{P}_c + \mathcal{P}_w) = 0 \tag{10}$$

$$\frac{\hbar_w}{\varepsilon_w}\,\mathcal{K}\frac{\partial \mathcal{P}_w}{\partial x} + \frac{\hbar_o}{\varepsilon_o}\,\mathcal{K}\frac{\partial \mathcal{P}_c}{\partial x} + \frac{\hbar_o}{\varepsilon_o}\,\mathcal{K}\frac{\partial \mathcal{P}_w}{\partial x} = 0 \tag{11}$$

Simplifying,

$$\mathcal{K}\frac{\partial \mathcal{P}_w}{\partial x}\left(\frac{\hbar_w}{\varepsilon_w} + \frac{\hbar_o}{\varepsilon_o}\right) + \frac{\hbar_o}{\varepsilon_o}\mathcal{K}\frac{\partial \mathcal{P}_c}{\partial x} = 0 \tag{12}$$

$$\mathcal{K}\frac{\partial \mathcal{P}_w}{\partial x} = -\frac{\frac{\hbar_o}{\varepsilon_o}\mathcal{K}\frac{\partial \mathcal{P}_c}{\partial x}}{\left(\frac{\hbar_w}{\varepsilon_w}+\frac{\hbar_o}{\varepsilon_o}\right)} \tag{13}$$

Substituting in equation (4)

$$\varphi\frac{\partial S_w}{\partial t} + \frac{\partial}{\partial x}\left(\frac{\hbar_w}{\varepsilon_w}\,\mathcal{K}\frac{\frac{\hbar_o}{\varepsilon_o}\mathcal{K}\frac{\partial \mathcal{P}_c}{\partial x}}{\frac{\hbar_w}{\varepsilon_w}+\frac{\hbar_o}{\varepsilon_o}}\right) = 0 \tag{14}$$

Using,

$$\frac{\partial \mathcal{P}_c}{\partial x} = \frac{\partial \mathcal{P}_c}{\partial S_w}\frac{\partial S_w}{\partial x}$$

We get,

$$\varphi\frac{\partial S_w}{\partial t} + \frac{\partial}{\partial x}\left(\frac{\frac{\hbar_w}{\varepsilon_w}\mathcal{K}\frac{\hbar_o}{\varepsilon_o}\frac{\partial \mathcal{P}_c}{\partial S_w}\frac{\partial S_w}{\partial x}}{\frac{\hbar_w}{\varepsilon_w}+\frac{\hbar_o}{\varepsilon_o}}\right) = 0 \tag{15}$$

According to Scheidegger [16],

$$\frac{\frac{\hbar_w \hbar_o}{\varepsilon_w \varepsilon_o}}{\frac{\hbar_w}{\varepsilon_w}+\frac{\hbar_o}{\varepsilon_o}} \approx \frac{\hbar_o}{\varepsilon_o} \tag{16}$$

Therefore, equation (15) reduces to,

$$\varphi\frac{\partial S_w}{\partial t} + \mathcal{K}\frac{\partial}{\partial x}\left(\frac{\hbar_o}{\varepsilon_o}\frac{\partial \mathcal{P}_c}{\partial S_w}\frac{\partial S_w}{\partial x}\right) = 0 \tag{17}$$

Scheidegger and Johnson [18] assume that both oil and water exhibit linear relative permeability.

$\hbar_w = S_w$

$\hbar_o = 1 - \alpha S_w$, where $\alpha = 1.11$ (18)

Mehta [4] indicates that capillary pressure can be expressed in terms of saturation as follows:

$\mathcal{P}_c = -\beta S_w$, where β is constant (19)

We obtain from equations (16), (17), and (18)

$$\varphi \frac{\partial S_w}{\partial t} = \frac{\hbar\beta}{\varepsilon_o} \frac{\partial}{\partial x}\left((1 - \alpha S_w)\frac{\partial S_w}{\partial x}\right) \quad (20)$$

The nonlinear partial differential equation in (20) describes the imbibition event. The first requirement is:

$S_w(x, 0) = A(x), 0 \le x \le l$ (21)

The boundary conditions are,

$S_w(0, t) = B(t), 0 < t \le 1,$ (22)

$S_w(l, t) = C(t), 0 < t \le 1$ (23)

Time $t > 0$ influences the water saturation at $x = 0$ and $x = l$, where $l \ll L$ and $x = l$ is near the common interface ($x = 0$). Use dimensionless parameters to convert equation (20) into its dimensionless form.

$$X = \frac{x}{l}, T = \frac{\hbar\beta}{\varphi\varepsilon_o L^2} t$$

Equation (20) is converted into,

$$\frac{\partial \mathrm{S_w}}{\partial \mathrm{T}} = \frac{\partial}{\partial \mathrm{X}}\left[(1 - \alpha \mathrm{S_w})\frac{\partial \mathrm{S_W}}{\partial \mathrm{X}}\right] \quad (24)$$

By modifying the initial and boundary conditions, we arrive at

$S_w(X, 0) = A(X), 0 \le X \le 1$ (25)

$S_w(0, T) = B(T), 0 < T \le 1,$ (26)

$S_w(l, T) = C(T), 0 < T \le 1$ (27)

Problem Solution

The Homotopy Analysis Method (HAM) is very useful for simulating imbibition processes in porous media, especially for the investigation of two-phase fluid displacement processes such as water-oil interactions. In counter-current imbibition, the governing equations are typically nonlinear partial differential equations that are not readily solvable using conventional analytical methods. HAM is an extremely powerful tool for obtaining accurate, convergent series solutions without having to assume small or large parameters. This flexibility proves extremely useful in modeling the complex behavior of saturation fronts, capillary-driven flow, and dynamic boundary conditions typical of imbibition phenomena. With HAM, researchers can derive explicit analytical solutions for fluid saturation profiles and flow rates, enabling one to better understand oil recovery efficiency and porous media performance optimization under actual reservoir conditions.

The detailed flow chart of HAM is shown in Fig. 2. [19]

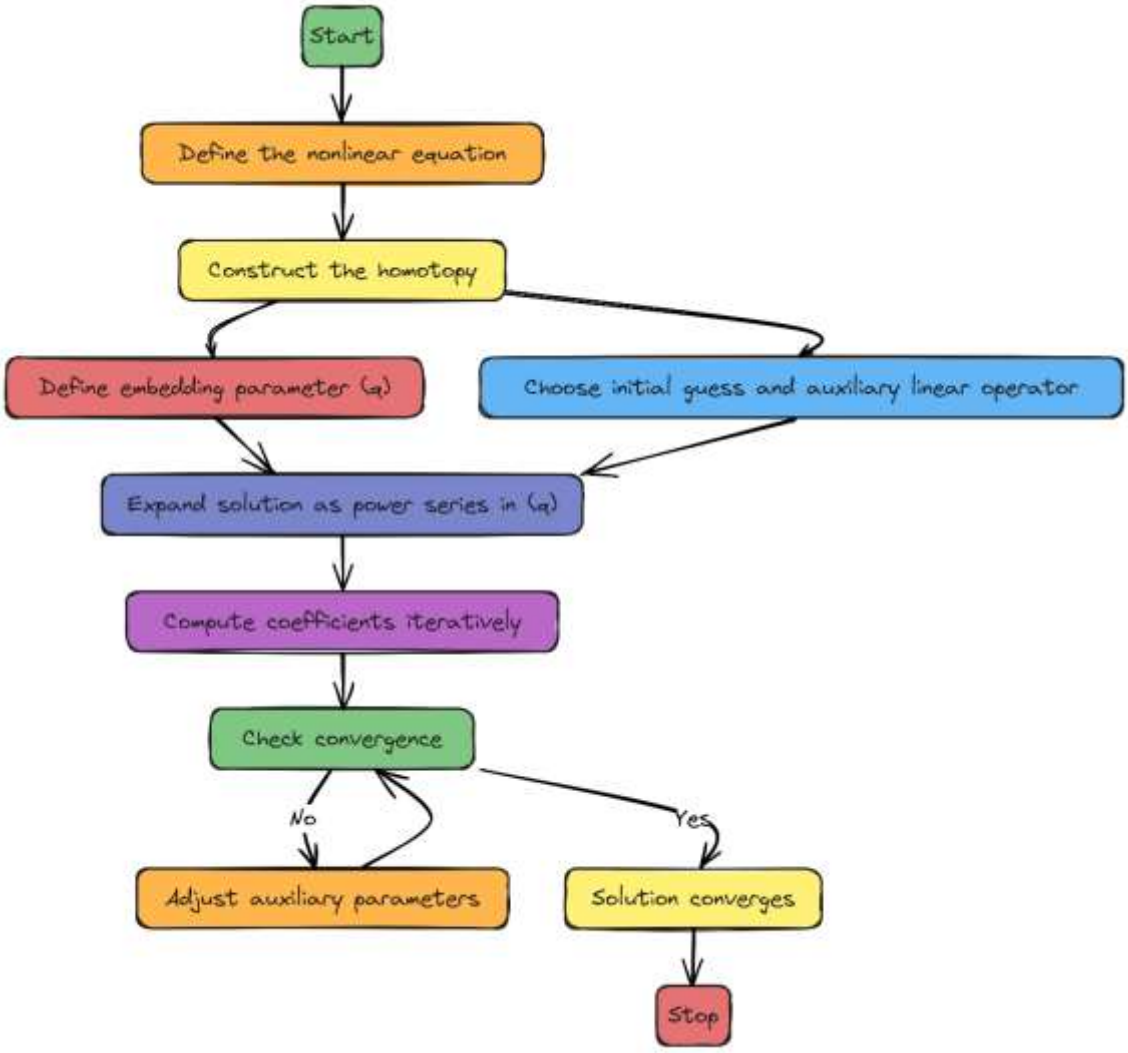

Fig. 2 : Flow chart of numerical method

In this section, we use HAM to solve Non-linear P.D.E. of equation (24) by taking the appropriate boundary conditions are as follows:

$$\left.\begin{aligned} S_w\,(0,T) = 0,\ 0 < T \le 1 \\ S_w\,(1,T) = \left(\tfrac{1+T}{3}\right), 0 < T \le 1 \end{aligned}\right\} \tag{28}$$

The Homotopy Analysis Method (HAM) was originally introduced by Liao [20] in his 1992 PhD thesis. Famed for its flexibility and potency, HAM has emerged as a very useful analytical method to solve a variety of nonlinear differential equations. In recent years, it has been applied successfully to many partial differential equations [21-29] and ordinary differential equations [30-32] and has illustrated its wide scope of applicability. One of the important characteristics of HAM is its convergence control parameter, i.e., c_0, that is essential for making sure that the series solution converges correctly. The best possible value of c_0 can be determined by studying the c_0 -curve, which proves useful in increasing the accuracy of derived solutions.

In addition, as per the given boundary conditions, HAM recommends selecting a suitable initial guess or initial approximation that closely matches the expected behavior of the solution as given in equation (29). This judicious selection also allows the homotopy series to converge very quickly and stably, thus recommending HAM as a very reliable method for solving complex nonlinear problems in scientific and engineering fields.

$$S_{w0}(X,T) = \left(\frac{2(X+TX^2)}{6}\right) \tag{29}$$

We select the auxiliary linear operator based on equation (24).

$$\mathfrak{L}[\varphi(X,T;\theta)] = \frac{\partial^2 \varphi(X,T;\theta)}{\partial X^2} \tag{30}$$

This satisfies the characteristic $\mathfrak{L}[\mathcal{A}x + \mathcal{b}] = 0$ where $\mathcal{A}$ and $\mathcal{b}$ are constants.

$$\mathfrak{N}\big(\varphi(X,T;\theta)\big) = \left(\frac{\partial^2 \varphi(X,T;\theta)}{\partial X^2}\right) - \alpha\varphi(X,T;\theta)\left(\frac{\partial^2 \varphi(X,T;\theta)}{\partial X^2}\right) - \alpha\left(\frac{\partial^2 \varphi(X,T;\theta)}{\partial X^2}\right)^2 - \left(\frac{\partial^2 \varphi(X,T;\theta)}{\partial T}\right) \tag{31}$$

The zeroth-order deformation equation was created by Liao [20].

$$(1-\theta)\mathfrak{L}\big[\varphi(X,T;\theta) - S_{w_0}(X,T)\big] = \theta c_0 \mathfrak{K}(X,T) N\big(\varphi(X,T;\theta)\big) \tag{32}$$

where $\theta \in [0,1]$ the embedding-parameter, $c_0 \neq 0$ the convergence control parameter, $\mathfrak{K}(X,T) \neq 0$ the auxiliary function.

When $\theta = 0$ and $\theta = 1$, Eq. (11) provided

$$\varphi(X,T;0) = S_{w_0}(X,T) \text{ and } \varphi(X,T;1) = S_w(X,T) \tag{33}$$

Thus as θ increases from 0 to 1, $\varphi(X,T;\theta)$ continuously deforms from the initial approximation $S_{w_0}(X,T)$ to the exact solution $S_w(X,T)$ of the Eq. (24).

Assume that the auxiliary linear operator, the initial approximation, the convergence control parameter and the auxiliary function are chosen so properly that the Maclaurin series of $\varphi(X,T;\theta)$ with respect to θ

$$\varphi(X,T;\theta) = S_{w_0}(X,T) + \sum_{m=1}^{\infty} S_{w_m}(X,T)\theta^m \tag{34}$$

$$\text{Where, } S_{w_m}(X,T) = \frac{1}{m!}\frac{\partial^m \varphi(X,T;\theta)}{\partial \theta^m}\Big|_{\theta=0} \tag{35}$$

Converges at $\theta = 1$. Thus we have solution

$$S_w(X,T) = S_{w_0}(X,T) + \sum_{m=1}^{\infty} S_{w_m}(X,T) \tag{36}$$

Define $\overrightarrow{\mathrm{S_{w_m}}(X,T)} = \{\mathrm{S_{w_0}}(\mathrm{X},\mathrm{T}), \mathrm{S_{w_1}}(\mathrm{X},\mathrm{T}), \ldots\ldots, \mathrm{S_{w_m}}(\mathrm{X},\mathrm{T})\}$. Differentiating the Eq. (32) m times with respect to the embedding-parameter θ and dividing them by $m!$ and then finally setting$\theta = 0$, we have the high-order deformation equation

$$\mathfrak{L}\left[S_{w_m}(X,T) - \chi_m S_{w_{m-1}}(X,T)\right] = c_0 \mathfrak{K}(X,T)\mathfrak{R}_m\left(\overrightarrow{S_{w_{m-1}}}\right) \tag{37}$$

Subject to the boundary conditions

$$S_{w_m}(0,T) = 0, S_{w_m}(1,T) = 0\,, m \geq 1 \tag{38}$$

Where,

$$\mathfrak{R}_m\left(\overrightarrow{S_{w_{m-1}}}\right) = \frac{1}{(m-1)!}\frac{\partial^{m-1}\mathfrak{N}\left(\varphi(X,T;\theta)\right)}{\partial\theta^{m-1}}\Big|_{\theta=0} \tag{39}$$

and $\chi_m = \begin{cases} 0\,, When\ m \leq 1 \\ 1\,, When\ m > 1 \end{cases}$ (40)

For simplicity, we assume that $\mathfrak{K}(X,T) = 1$.Therefore, solving linear ordinary differential equations (37) is straightforward. As a result, the general solution to the high-order deformation equation (37) is

$$S_{w_m}(X,T) = \chi_m S_{w_{m-1}}(X,T) + c_o \iint \mathfrak{R}_m\left(\overrightarrow{S_{w_{m-1}}}\right)dxdx + \mathcal{A}x + \mathcal{b} \tag{41}$$

where $\mathcal{A}$ and $\mathcal{b}$ are constants or functions of T. Hence the approximate analytical solution of the Eq. (24) is as

$$\mathrm{S_w}(\mathrm{X},\mathrm{T}) = \left(\frac{2\left(\mathrm{X}+\mathrm{TX}^2\right)}{6}\right) + \mathrm{c_0}\left[\mathrm{X}\left(\frac{\alpha}{18} + \frac{\alpha\mathrm{T}}{9} + \frac{\alpha\mathrm{T}^2}{18} - \frac{5}{18}\right) + \mathrm{X}^2\left(\frac{1}{3} - \frac{\alpha\mathrm{T}^2}{18}\right) - \mathrm{X}^3\left(\frac{1}{18} + \frac{\alpha\mathrm{T}}{9}\right) - \frac{\alpha\mathrm{X}^4}{18}\right] \ldots\ldots\ldots \tag{42}$$

Results and Discussion

The control parameter c_0 of convergence in the convergence characteristic of series solutions derived by Homotopy Analysis Method (HAM) is instrumental. In this research, the convergence of series $S_{W_{XX}}(0,1)$ and $S_{W_{XX}}(0,0.2)$ is studied in terms of changes in c_0 As per the suggestion of Liao [15], it is found that both $S_{W_{XX}}(0,1)$ and $S_{W_{XX}}(0,0.2)$ converge to the same values throughout the range of c_0 where the solution is stable. The curves defining $S_{W_{XX}}(0,1)$ and $S_{W_{XX}}(0,0.2)$ against c_0 are referred to as c_0-curves [19, 26], and are crucial to identify the valid region of convergence for c_0. The presence of a horizontal segment in the c_0 curves, as proposed by Liao [30-32], represents the interval in which the series converge suitably.

Figures 3 and 4 show the c_0 curves for obtained with Mathematica for the 10th -order and 20th -order approximations, respectively. In the two figures, the solid lines are the two series'

convergence profiles. As can be easily seen from these plots, there is a quite large horizontal part where both curves are almost flat, showing that the solutions in that range are stable. Particularly, the valid range of convergence is found to be about $c_0 \in [-1.5,0.3]$. Beyond these limits, the curves show sharp oscillations, which is an indication of the loss of convergence or instability in the solution. In comparing Figures 3 and 4, one sees that raising the order of the approximation extends the flatness and width of the horizontal segment, corroborating the enhanced convergence and accuracy of the HAM solutions at higher orders.

Hence, the examination of the c_0-curves not only confirms the validity of the Homotopy Analysis Method for the problem under consideration but also sheds key light upon choosing an optimum c_0 value to ensure accurate and stable solutions. The determination of the admissible region of c_0 values is essential for practical purposes, guaranteeing that the series approximations employed in the analysis of the countercurrent imbibition effect are convergent and physically acceptable.

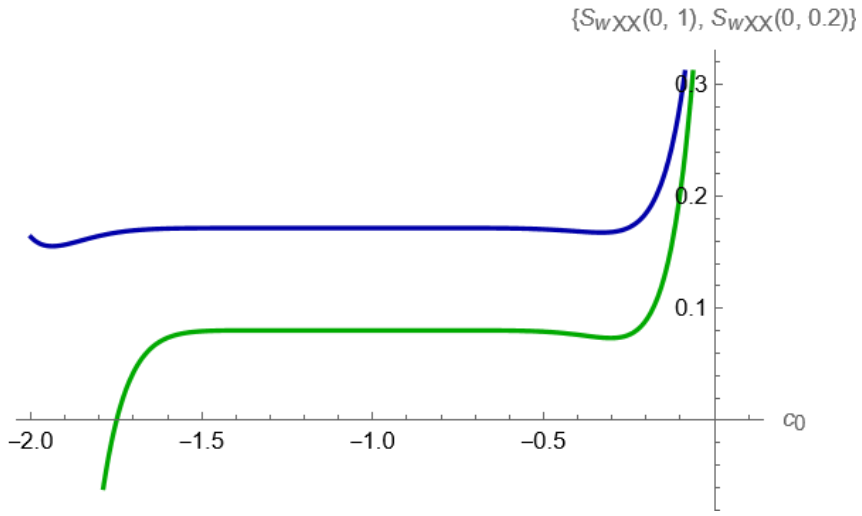

Fig.3 The c_0 Curve of $S_{w_{XX}}(0,1)$ (Solid Line) and $S_{w_{XX}}(0,0.2)$ (Solid Line) for 10th order Approximation

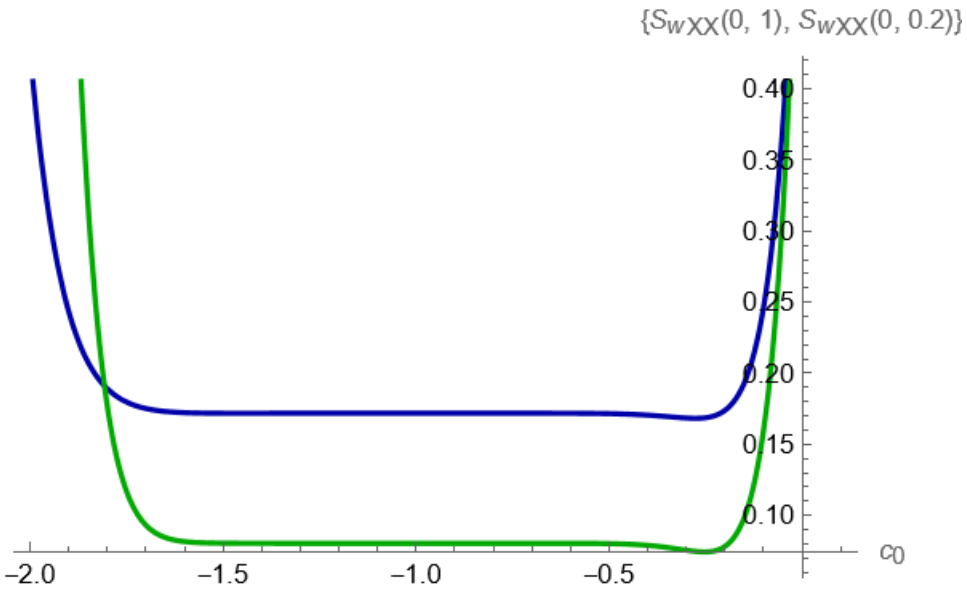

Fig.4 The c_0 Curve of $S_{w_{XX}}(0,1)$ (Solid Line) and $S_{w_{XX}}(0,0.2)$ (Solid Line) for 20th order Approximation.

Tables 1 and 2 show the numerical values of the saturation profile $S_W(X,T)$ from solving equation (42) by the Homotopy Analysis Method (HAM) with a convergence control parameter $c_0 = -1$. Table 1 is for the 10th-order approximation, and Table 2 is for the 20th-order approximation. The saturation values are calculated at different spatial positions $X \in [0,1]$ and at specified times$T = 0.2,0.4,0.6,0.8,1.0$. As anticipated, the saturation S_W grows with both distance X and time T, marking the increasing imbibition of the wetting fluid into the porous medium. Far from the boundary, at $X = 0$, the saturation is zero for all times, in accordance with the problem's boundary conditions. As one moves away from the boundary, the saturation rises uniformly, tracing the moving front of fluid invasion into the medium.

Observing the results for the 10th-order (Table 1) and the 20th-order (Table 2) approximations and comparing them, it can clearly be seen that the values match quite closely, showing the trustworthiness and convergence of solutions obtained using HAM even with lower orders of approximation. A small variation within the decimal points can be found, especially within the intermediate times and distances, illustrating the superior accuracy of the higher-order solution. The table consistency also justifies the selection of $c_0 = -1$ within the convergence region specified, as obtained from the analysis of the c_0-curve. Also, the smooth and monotonically increasing behavior of $S_W(X,T)$ with respect to both X and T justifies the physical applicability of the simulated imbibition process, establishing that the suggested mathematical framework correctly describes the fluid displacement dynamics in a uniform porous medium.

X	T=0.2	T=0.4	T=0.6	T=0.8	T=1.0
0	0	0	0	0	0

0.1	0.027337	0.03125	0.034709	0.037714	0.0402607
0.2	0.055779	0.063864	0.071045	0.077305	0.0826283
0.3	0.085684	0.098232	0.109431	0.119233	0.127596
0.4	0.11749	0.134839	0.150408	0.164099	0.175822
0.5	0.151739	0.174309	0.194692	0.212715	0.228211
0.6	0.189125	0.217468	0.243263	0.26623	0.286081
0.7	0.230572	0.265467	0.297548	0.32638	0.351493
0.8	0.277371	0.320006	0.359771	0.396032	0.428035
0.9	0.331452	0.383828	0.433835	0.480667	0.523194
1	0.396	0.462	0.528	0.594	0.66

Table 1: Numerical Value of Solution $S_w(X,T)$ when $c_0 = -1$ for 10thorder approximation

X	T=0.2	T=0.4	T=0.6	T=0.8	T=1.0
0	0	0	0	0	0
0.1	0.0273367	0.0312496	0.0347094	0.03771	0.04026
0.2	0.0557786	0.0638643	0.0710455	0.07731	0.08263
0.3	0.0856842	0.0982323	0.109431	0.11923	0.1276
0.4	0.11749	0.134839	0.150408	0.1641	0.17582
0.5	0.151739	0.174309	0.194692	0.21272	0.22821
0.6	0.189125	0.217468	0.243264	0.26623	0.28608
0.7	0.230572	0.265467	0.297549	0.32638	0.35149
0.8	0.277371	0.320006	0.359773	0.39603	0.42803
0.9	0.331452	0.383828	0.433836	0.48067	0.52318
1	0.396	0.462	0.528	0.594	0.66

Table 2: Numerical Value of Solution $S_w(X,T)$ when $c_0 = -1$ for 20thorder approximation

The graphical representations given in Figures 5 and 6 present a clear picture of the variation of the saturation profile$S_W(X,T)$ because of the convergence control parameter$c_0 = -1$. Figure 5 shows the variation of $S_W(X,T)$ as a function of the spatial coordinate X for various fixed values of time $T = 0.2,0.4,0.6,0.8,1.0$. It is seen that for a specific time, the saturation rises nonlinearly with distance, reflecting the continuous imbibition of the wetting phase into the porous medium. The slope of the plots steepens with rising T, corresponding to the deeper fluid intrusion at longer times. Figure 6 illustrates the time evolution of $S_W(X,T)$ for a given spatial location $X = 0.2,0.4,0.6,0.8,1.0$. It is apparent that at any distance, the saturation rises systematically with time, displaying a typical imbibition process by which the wetting phase saturation rises as time evolves. The two figures collectively demonstrate the homotopy analysis method's ability to capture the realistic spatial-temporal behavior of the saturation front in porous media.

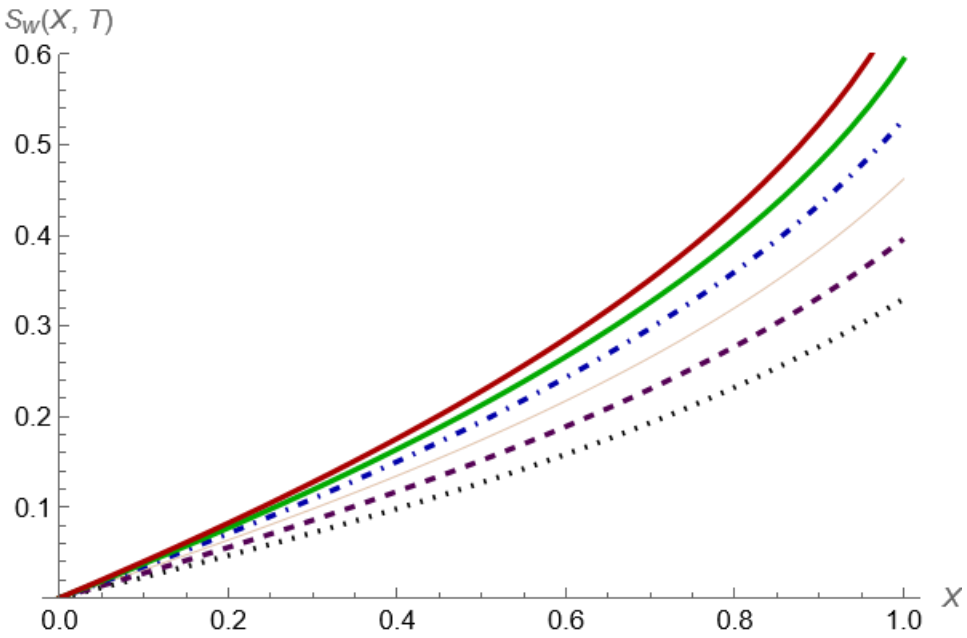

Fig.5 Solution $S_w(X,T)$ v/s distance X at a constant time T=0.2,0.4,0.6,0.8,1.0

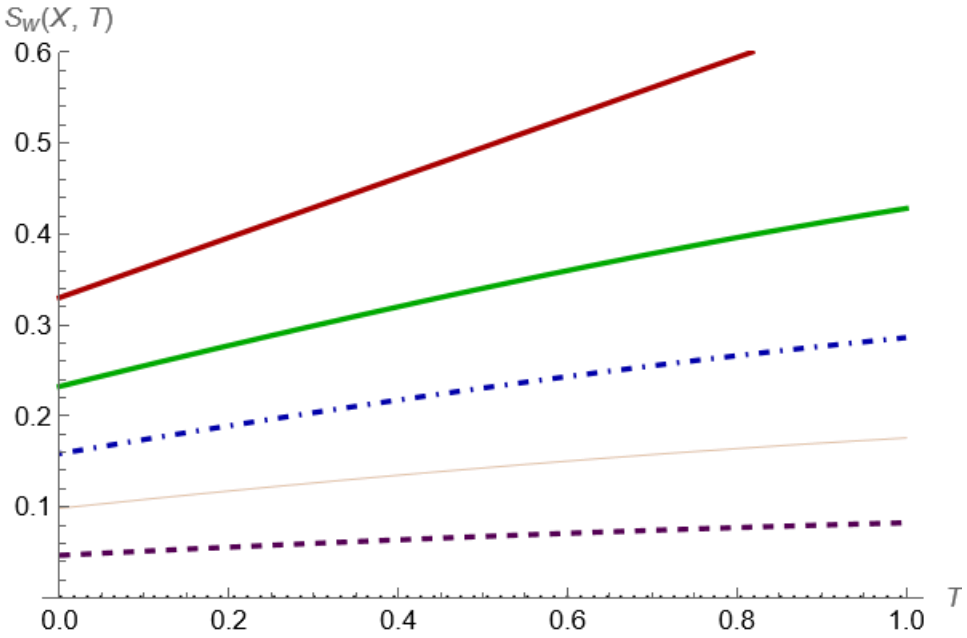

Fig.6 Solution $S_w(X,T)$ v/s time T for fixed distance X =0.2,0.4,0.6,0.8,1.

Conclusions

In the present work, the convergence properties of series solutions obtained by means of the Homotopy Analysis Method (HAM) were thoroughly investigated through the c_0 -behavior of

the convergence control parameter. The examination of the c_0-curves for $S_{W_{XX}}(0,1)$ and $S_{W_{XX}}(0,0.2)$ displayed plainly a stable broad horizontal interval in the interval $c_0 \in [-1.5,0.3]$, which ascertained the reliability and robustness of the HAM solutions within this interval. Figures 3 and 4 of the c_0-curves for 10th- and 20th-order approximations also supported further that higher-order approximation improves the stability and convergence interval of the solution. The common horizontal segments observed testified to the adequacy of HAM in tackling difficult nonlinear problems such as countercurrent imbibition, which was in conformity with the theoretical expectations of Liao.

Furthermore, numerically computed saturation profiles $S_W(X,T)$ at different spatial and temporal coordinates, e.g., Tables 1 and 2, confirm the validity and accuracy of the technique. Comparison between 10th and 20th-order solutions shows that even low-order solutions are extremely accurate with zero deviation, and higher-order solutions are even more accurate. Figures 5 and 6 further corroborate this conclusion by visually exhibiting the expected physical behavior: the saturation increases monotonically with both space and time, precisely simulating the imbibition phenomenon in a homogeneous porous medium. Consistency across tables and graphical findings highlight that the mathematical setup and selection of $c_0 = -1$ are suitable for the modeling of realistic fluid invasion processes.

Lastly, the graphical representations given thoroughly portray the physical phenomena in question with all figures properly corresponding to theory expectations and experimental observations of imbibition behavior. The nonlinear growth of saturation with distance at a given time and systematic growth with time at a given spatial point, as in Figures 5 and 6, capture the progressive penetration of the wetting phase, fulfilling the boundary conditions and physical expectation of porous media flow. In summary, the convergence analyses, numerical solutions, and graphical verifications all jointly demonstrate that the Homotopy Analysis Method, with appropriately chosen parameters, presents a powerful, accurate, and physically sound tool for solving countercurrent imbibition problems in porous media.

Conflict of Interest

The authors declare that they have no conflict of interest.

Author Contributions

The author contributed to the conceptualization, mathematical modeling, analytical derivations, computational simulations, data interpretation, and manuscript preparation of this research work. All aspects of the study, including literature review, problem formulation, implementation of the Homotopy Analysis Method (HAM), result analysis, and manuscript drafting, were performed independently by the author.

Data Availability Statement

The data supporting the findings of this study are available within the article itself. Any additional numerical data, computational codes, or simulation files generated during the current study are available from the corresponding author upon reasonable request.

Funding Statement

The author declares that no financial support, grants, or funding from any external agency, commercial, or non-commercial source was received for conducting this research and preparing this manuscript.

Acknowledgement

The author sincerely acknowledges and expresses heartfelt gratitude to all the anonymous reviewers for their valuable suggestions and constructive feedback, which significantly improved the quality of this paper. Special thanks to Ms. Tejal Nagar, Mr. Ajay Yadav, Mr. Amit Upadhyay, and Mr. Vikas Kori for their continuous encouragement, insightful discussions, and technical support, which greatly helped in enhancing the quality and clarity of the present work.

Nomenclature

Notation	Meaning
$\mathcal{V}_w$	The seepage velocity of water in the wetting phase [m/s]
$\mathcal{V}_o$	The seepage velocity of the oil in the non-wetting phase [m/s]
$\mathcal{K}$	Effectiveness of the porous medium's permeability [m^2]
$\mathcal{k}_w$	The porous medium's intrinsic permeability to the wetting phase [m^2]
$\mathcal{k}_o$	The porous medium's intrinsic permeability to the non-wetting phase [m^2]
$\mathcal{P}_w$	The pressure of the water in the wetting phase [Pa]
$\mathcal{P}_o$	The pressure of the oil in the non-wetting phase [Pa]
ε_w	water's constant kinematic viscosity
ε_o	oil's constant kinematic viscosity
φ	The porous medium's total porosity (volume of voids / total volume)
S_w	Saturation of the wetting phase (water) (volume of water / volume of voids)
S_o	Saturation of the non-wetting phase (oil) (volume of oil / volume of voids)

References

1. Yang, L., Li, M., Zhang, H. et al. Phase-Field Simulation of Counter-Current Imbibition and Factors Influencing Recovery Efficiency. Transp Porous Med 151, 2727–2743 (2024). https://doi.org/10.1007/s11242-024-02134-4.

2. Zhou, Y., Guan, W., Zhao, C., Zou, X., He, Z., Zhao, H. Spontaneous imbibition behavior in porous media with various hydraulic fracture propagations: A pore-scale perspective. Advances in Geo-Energy Research, 2023, 9(3): 185-197. https://doi.org/10.46690/ager.2023.09.06
3. Shuai Yuan, Fujian Zhou, Mengqi Ma, Zhenglong Sun, Jingtao Zhang, Tianbo Liang, Junjian Li; An experimental study on the imbibition characteristics in heterogeneous porous medium. Physics of Fluids 1 November 2023; 35 (11): 113604. https://doi.org/10.1063/5.0171681
4. Xu, F., Jiang, H., Liu, M., Jiang, S., Wang, Y., & Li, J. (2023). NMR-Based Analysis of Fluid Occurrence Space and Imbibition Oil Recovery in Gulong Shale. Processes, 11(6), 1678. https://doi.org/10.3390/pr11061678
5. Parikh, A. K., Mehta, M. N., & Pradhan, V. H. (2013). Mathematical Model and Analysis of Counter-Current Imbibition in Vertical Downward Homogeneous Porous Media. Journal of Advances in Mathematics and Computer Science, 3(4), 478–489.
6. Gohil, V. P., & Meher, R. (2019). Effect of Viscous Fluid on the Counter-Current Imbibition Phenomenon in Two-Phase Fluid Flow Through Heterogeneous Porous Media with Magnetic Field. Iranian Journal of Science and Technology, Transactions of Science, 43(1), 1799–1810.
7. Suo, S., Liu, M., & Gan, Y. (2018). Modelling Imbibition Processes in Heterogeneous Porous Media. arXiv preprint arXiv:1805.07864.
8. Zotelle, A.C., Souza, A.W.Q., Pires, P.J.M. et al. Viscosity ratio effects on fluid displacement pattern and recovery efficiency on porous media. J Braz. Soc. Mech. Sci. Eng. 45, 149 (2023). https://doi.org/10.1007/s40430-023-04041-z
9. Liu Y, Zou J, Lan X, Gao S, Zhang L and He X (2023) Research on imbibition effect of surfactant fracturing fluid in offshore reservoirs with low permeability and high temperature. Front. Energy Res. 11:1297738. doi: 10.3389/fenrg.2023.1297738
10. Zhang, J., Huang, H., Zhang, M., & Wang, W. (2023). Experimental investigation of nanofluid enhanced oil recovery by spontaneous imbibition. In RSC Advances (Vol. 13, Issue 24, pp. 16165–16174). Royal Society of Chemistry (RSC). https://doi.org/10.1039/d2ra06762e
11. Meng, M., Zhang, Y., Yuan, B., Li, Z., & Zhang, Y. (2023). Imbibition Behavior of Oil-Saturated Rock: Implications for Enhanced Oil Recovery in Unconventional Reservoirs. In Energy & Fuels (Vol. 37, Issue 18, pp. 13759–13768). American Chemical Society (ACS). https://doi.org/10.1021/acs.energyfuels.3c02501
12. Wang, F., Wang, L., Jiao, L., Liu, Z., & Yang, K. (2023). Experimental Mechanism for Enhancing Oil Recovery by Spontaneous Imbibition with Surfactants in a Tight Sandstone Oil Reservoir. In Energy & Fuels (Vol. 37, Issue 12, pp. 8180–8189). American Chemical Society (ACS). https://doi.org/10.1021/acs.energyfuels.3c00525

13. Li, Y. Analytical Solutions for Linear Counter-Current Spontaneous Imbibition in the Frontal Flow Period. Transp Porous Med 86, 827–850 (2011). https://doi.org/10.1007/s11242-010-9656-y
14. Tavassoli, Z., Zimmerman, R.W. & Blunt, M.J. Analytic Analysis for Oil Recovery During Counter-Current Imbibition in Strongly Water-Wet Systems. Transp Porous Med 58, 173–189 (2005). https://doi.org/10.1007/s11242-004-5474-4
15. Mason, G., Fischer, H., Morrow, N.R. et al. Spontaneous Counter-Current Imbibition into Core Samples with All Faces Open. Transp Porous Med 78, 199–216 (2009). https://doi.org/10.1007/s11242-008-9296-7
16. Scheidegger, A.E. (1960). The Physics of Flow Through Porous Media (3rd ed.). University of Toronto Press. https://doi.org/10.3138/9781487583750
17. Mehta, M.N. (1978). Asymptotic Expansion in Fluid Flow Through Porous Media (Doctoral dissertation). S.G. University, Surat, India.
18. Scheidegger, A. E., & Johnson, E. F. (1961). The Statistical Behavior Of Instabilities In Displacement Processes In Porous Media. In Canadian Journal of Physics (Vol. 39, Issue 2, pp. 326–334). Canadian Science Publishing. https://doi.org/10.1139/p61-031
19. Mittal, A.S., Kori, V. Impact of Dufour-Soret Diffusion and Chemical Reactivity on Darcy-Forchheimer MHD Nanofluid Flow Over a Variable-Thickness Elastico-Viscous Sheet. *Int. J. Appl. Comput. Math* **11**, 28 (2025). https://doi.org/10.1007/s40819-025-01834-9
20. Liao, S.J. (1992). The Proposed Homotopy Analysis Technique for Solving Nonlinear Problems (Doctoral dissertation). Shanghai Jiao Tong University, Shanghai, China.
21. Roy, K. (2024). Dissipation Induced Instability in Porous Medium Using Brinkman Model: Thermal Non-Equilibrium Effect. Physics of Fluids, 36(1), 014128. https://doi.org/10.1063/5.0186872
22. Joshi, M.S., Desai, N.B., & Mehta, M.N. (2011). Analytical Solution to the Countercurrent Imbibition Phenomenon in Fluid Flow Through Homogeneous Porous Media. International Journal of Applied Mathematics and Mechanics, 7(11), 21–32.
23. Zakeri, S., Hazlett, R., & Babu, K. (2023). An Analytic Solution for Counter-Current Spontaneous Imbibition in Porous Media by the Perturbation Method. Journal of Hydrology, 620, 129181. https://doi.org/10.1016/j.jhydrol.2023.129181
24. Velasco-Lozano, M., & Balhoff, M.T. (2021). A Semi-Analytical Solution for Countercurrent Spontaneous Imbibition in Water-Wet Fractured Reservoirs. Transport in Porous Media, 138, 77–97. https://doi.org/10.1007/s11242-021-01591-5
25. Cheng, Z., Tong, S., Shang, X., Yu, J., Li, X., & Dou, L. (2024). Lattice Boltzmann simulation of counter-current imbibition of oil and water in porous media at the equivalent capillarity. In AIP Advances (Vol. 14, Issue 8). AIP Publishing. https://doi.org/10.1063/5.0219191

26. Patel, M.A., & Desai, N.B. (2017). Application of Homotopy Analysis Method to Solve Nonlinear Partial Differential Equation Related to Fluid Flow Through Porous Medium. International Journal of Computer & Mathematical Sciences, 6(5), 1–6 ISSN 2347-8527.
27. Iyiola, O.S., & Folarin, S.B. (2014). Approximate Analytical Study of Fingero-Imbibition Phenomena of Time-Fractional Type in Double Phase Flow Through Porous Media. European Journal of Pure and Applied Mathematics, 7(2), 210–229 ISSN 1307-5543.
28. Parikh, A.K., Mehta, M.N., & Pradhan, V.H. (2013). Generalized Separable Solution for the Counter-Current Imbibition Phenomenon in a Homogeneous Porous Medium in the Horizontal Direction. The International Journal of Engineering and Science, 2(1), 220–226.
29. Sharma, A., & Parikh, A.K. (2023). Semi Analytic-Numerical Solution of Imbibition Phenomenon in Homogeneous Porous Medium Using Hybrid Differential Transform Finite Difference Method. Communications in Mathematics and Applications, 14(3), 1199–1213.
30. Liao, S.J. (2003). Beyond Perturbation: Introduction to the Homotopy Analysis Method. Chapman and Hall/CRC Press.
31. Liao, S.J. (2012). Homotopy Analysis Method in Nonlinear Differential Equations. Higher Education Press & Springer-Verlag.
32. Nagar, Tejal; Patel, Harshad; Mittal, Akhil; and Kori, Vikas (2025). (SI14-15) Heat Source/Sink and Chemical Reaction Effects on Micropolar MHD Nano Fluid Flow in Stretching/Shrinking Sheet, Applications and Applied Mathematics: An International Journal (AAM), Vol. 20, Iss. 3, Article 6.